31st Congress of the International Council
of the Aeronautical Sciences

Belo Horizonte, Brazil; September 09-14, 2018

FLIGHT PERFORMANCE OF STEERABLE CRUCIFORM PARACHUTE SYSTEMS

Shawn M. Herrington* , Travis D. Fields* , and Oleg A. Yakimenko**
*University of Missouri-Kansas City , **Naval Postgraduate School

Keywords: *cruciform parachute, system identification, wind-tunnel testing, steering control*

Abstract

This paper discusses the development and testing of a steerable aerial delivery system based on an inexpensive cruciform canopy which can be used to deliver critical supplies to remote locations during humanitarian relief and other missions. Extensive experiments with a 1.5 m diameter parachute system were conducted in the 20-foot Vertical Spin Tunnel at the NASA Langley Research Center in Hampton, Virginia. Experimental data were used for system identification in order to model the dynamics in both pitch and yaw. This allowed development of a heading stabilizing controller to support a novel precision guidance scheme which was subsequently further evaluated in a series of outdoor drop tests from both manned and unmanned aircraft. Finally, two precision guidance schemes were evaluated with data collected from outdoor drop testing.

1 Introduction

Precision aerial delivery is concerned with the timely delivery of critical supplies to locations that are difficult or impossible to access by other means. Extensive research had been conducted in the early 2000's into autonomous steeerable guided ram-air parafoil systems which resulted in several systems being fielded. These systems offer large standoff distances as well as the capability to delivery supplies within 50 m to 100 m of the desired impact point on the ground [1]. Unfortunately, these systems are otherwise prohibitively expensive and that is why the vast majority of air cargo is still delivered by low-cost unguided parachute systems.

In the case of unguided drops; however, due to unpredictable and potentially adverse wind conditions, cargo risks being lost or otherwise unrecoverable if the airdrops are conducted from high altitudes. Conversely, airdrops conducted close to the ground to minimize the effects of the wind leave aircraft vulnerable to terrain and possibly hostile entities in and around the desired impact point.

The work presented herein focuses on the development of a system representing a hybrid approach to precision aerial delivery. Utilizing probably the least expensive parachute design and simple control scheme realized by a low-cost aerial guidance unit (AGU), constitutes a system that is only marginally more complex than unguided delivery systems but assures, impact point landing accuracy close to that of ram-air parafoil systems. This represents a substantial improvement over traditional aerial delivery by unguided parachute.

The paper is organized as follows. Section Section 2 proceeds with a brief description of the cruciform parachute based aerial delivery system followed by Section 3 which presents test objectives and methodology. The results of the wind tunnel and real airdrop testing are discussed in Section 4. The paper ends with conclusions.

2 Cruciform Parachute Systems

Cruciform, or cross, parachute systems are created by overlaying two rectangular panels of fabric as shown in Fig. 1 [2]. Their aerodynamics have been extensively studied in the past [3, 4, 5, 6, 7, 8]. Enabling steering control for such a system involves shortening or lengthening (deflecting) the suspension lines attached to the inner corners on a pair of adjacent panels. By pulling in the corner of one panel (asymmetrical deflection), a rotation about the vertical axis (yaw rotation) is produced. By dynamically actuating the suspension line affixed to the adjacent corner, the yaw rotation can be reversed or stopped. If both suspension lines are deflected by the same amount (symmetrical deflection), then the system tends to stabilize at a non-zero angle of attack which enables gliding rather than vertical descent. Even though the glide ratio (defined as a relative horizontal airspeed per unit of the descent rate) is relatively small, on the order of $1:0.25$ to $1:0.50$, it still creates an opportunity for precision aerial delivery.

Fig. 1 : Steerable cruciform parachute system during outdoor flight-testing

A few studies have investigated the potential of utilizing cruciform parachutes for horizontal glide. Potvin et al. [8] used fixed remotely-piloted asymmetric deformations trying to maximize glide ratio by changing parachute planform. Fields et al. developed an autonomously controllable system, utilizing a fixed basic planform with a $4:1$ aspect ratio (AR), and a testing technique that allowed them to obtain a conservative estimated glide ratio of approximately 0.3:1 [9]. However, the prior research into cruciform parachute systems faced difficulties in controlling the cruciform parachute based system when exposed to large and unpredictable wind disturbances when testing outdoors. The focus of the work herein is on the wind-tunnel based controller tuning and associated outdoor flight test verification.

3 Control Strategy and Test Methodology

This section presents the test methodology starting with a brief description of AGU hardware and software architecture followed by a discussion of wind tunnel and outdoor flight test setups. The objective of the wind tunnel testing was to tune the parameters of the controller in order to assure steady glide performance. Once a desirable performance has been achieved, the tuned controller was tested during real the real airdrop test campaign, which also included evaluation of two different guidance strategies.

3.1 AGU Hardware

The AGU was designed to use commercially available components wherever possible. This was done to facilitate the rapid and inexpensive development of an experimental platform. Suspension line deflection is accomplished with a large hobbyist sail boat winch servo capable of up to 0.48m deflection. All state estimation and actuator control was carried out with a microcomputer (Raspberry Pi 3) coupled with an inertial measurement unit shield (Emlid Navio2). The latter includes IMU, GPS, and barometric altitude sensors. The payload container shown in Fig. 1 with the AGU inside was loaded with 1-2kg of ballast (varied to yield different parachute loading), resulting in a total payload mass of approximately 5kg. The descriptive characteristics for the tested parachute are provided in Table 1.

Table 1: Cruciform canopy characteristics

Diameter	Panel AR	Parachute Area
1.75 m	3.0	1.35 m^2

3.2 Control System

A proportional-integral-derivative (PID) controller was utilized to stabilize the yaw angle of the parachute. In Eq. (1), λ is the actuator command and the error is computed as shown in Eq. (2) where Ψ is the yaw angle.

$$\lambda = K_pe + K_i \int e, dt + K_d \dot{e} \tag{1}$$

$$e = \Psi_{\text{des}} - \Psi_{\text{meas}} \tag{2}$$

A PID controller was chosen because of the simplicity of implementation on the chosen hardware.

3.3 Vertical Spin Tunnel Testing

Developmental test and evaluations of the cruciform-canopy-based system were performed in the NASA Langley 20-foot Vertical Spin Tunnel. The test setup is visualized in Fig. 2. The payload container was connected via swivel to a rigid mounting point in the wind tunnel. This enabled rotation of the complete parachute/payload system with relatively minimal side translation. In order to maintain tension on the anchor mechanism the wind tunnel was operated slightly above the terminal velocity of the parachute/payload.

Fig. 2 : Cruciform parachute during spin tunnel testing

The relative motion of the canopy about the payload was estimated using photogrammetry methods after the tests based on video data collected by an upward facing camera residing within the AGU. A frame capture from a typical upward facing video is shown in Fig. 3. This example shows positive identification of the two marker points adhered to the canopy. The image processing procedure involved first identifying the center marker, then centering and cropping the image relative to that marker. Next the other marker was identified and the angle between the markers relative to the frame was identified.

Fig. 3 : Frame capture from video used for photogrammetry

3.4 Guidance Strategies

Two guidance schemes have been evaluated in outdoor flight testing. The first of these schemes is known as persistent point-toward-target (PTT) navigation. By always commanding the system heading to point along a vector from the current position to the target, perfect impact point accuracy can be guaranteed as long as the vehicle can turn in place and is released within the parachute's gliding capability. The cruciform parachute requires finite time to turn (parachute size dependent), thereby limiting the accuracy of the PTT approach. However, the PTT guidance strategy does not require any prior knowledge about the wind conditions in the drop zone significantly simplifying aerial delivery operations. If the winds are weak and the system is dropped with a reasonable standoff distance from the impact point, then the system will arrive at the target zone with improved accuracy over a ballistic system deployed at the same release point. In general however, solving the precision airdrop problem makes use of an estimate of the wind conditions in the drop zone since the wind conditions can easily overpower the control authority of the parachute system. This is especially true for the cruciform parachute system tested in this study which can only penetrate a prevailing wind of approximately $2.5\,\mathrm{m/s}$.

The second guidance scheme is known as waypoint navigation (WPN). For this strategy a trajectory is generated which represents the ballistic trajectory given the forecast wind conditions. The ballistic trajectory is that trajectory which would be followed by a non-guided but otherwise similar system in order to arrive exactly at the desired impact point. The generated trajectory contains both ground track (latitude and longitude) and altitude information. The coordinates corresponding to the maximum altitude for a given trajectory is known as the computed aerial release point (CARP). This is the point from which the system should be dropped to yield the most robustness in the presence of release location errors and inaccurate wind forecast data.

The continuous descent trajectory is sampled at uniform altitude intervals in order to develop the altitude dependent waypoints to be uploaded to the AGU. During an airdrop, the system heading is commanded to point toward the active waypoint which is dependent on the current system altitude. When each successive altitude threshold is met, a new waypoint becomes active. This routine continues until the final altitude layer is reached at which time the active waypoint is the same as the desired impact point on the ground.

3.5 Flight Testing

Outdoor tests utilized the specially equipped DJI Matrice 600 lifting platform Fig. 4, Gryphon Dynamics heavy lift octocopter platform, UH-60 Blackhawk helicopter, and a Short SC.7 Skyvan fixed wing aircraft.

For each sortie, the test article includes one steerable cruciform system and a separate dropsonde. The dropsonde parachute is an uncontrolled simple flat circular parachute reefed to match the descent rate of the cruciform parachute as closely as possible. The dropsonde AGU contains a GPS logging device which records the translational position in 3-dimensional space at 1 Hz. For all flight testing, the aircraft was piloted near the CARP both the steerable system and the dropsonde were released. During many tests the CARP was manually determined by the ground crew or pilots (without consideration of the forecast wind data).

After release of the guided parachute, the AGU steers the system toward the target while the dropsonde falls according to the wind. Once the dropsonde is recovered, the GPS ground track is downloaded and used to create a smooth continuous ground track via interpolation. The generated continuous GPS track includes a continuous altitude vector which can be used to scale the effect of the wind to match a system with a different descent rate. To this end, the average descent rate of the tested scaled cruciform parachute system is $6.7\,\mathrm{m/s}$ whereas the dropsonde descent rate, though matched to the cruciform system by reefing, varies from drop-to-drop. A ratio of the measured GPS descent rate and the average measured cruciform system descent rate is used to stretch the GPS ground track to account for a slower descending parachute and payload system or shrink the GPS ground track to account for a faster descending parachute and payload system.

4 Results and Discussion

This section presents the results of wind-tunnel testing and real airdrop testing, highlighting all the findings.

4.1 Vertical Wind Tunnel Testing

Prior work by Potvin demonstrated that the glide tendency could be modified by altering the length

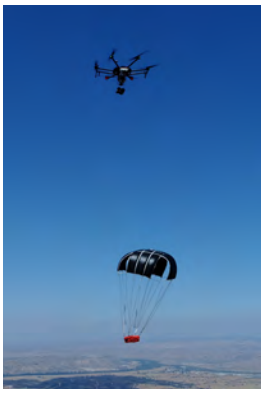

Fig. 4 : DJI Matrice 600 Lifting Platform

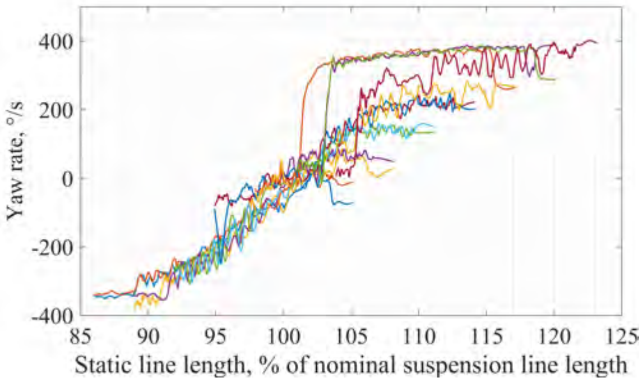

Fig. 5 : Heading rate vs. amount of dynamic line deflection

of the control lines [8]. However, no data had previously been collected which investigated what effect increasing or decreasing glide trim had on the heading rate dynamics of the system. To study the effect of suspension line length on the heading dynamics, the length of the dynamic line was commanded to sweep slowly from the minimum length (shorter than the static line length) to the maximum (longer than the static line length). The static line deflection was changed to a different fixed value prior to each experiment. Data from these experiments was used to characterize the general shape of the system response curve in terms of varying static line deflection as well as to study the maximum possible heading change rate for a given set of conditions.

Results showing the relationship between heading rate and static line length are presented in Fig. 5. Each line represents a different experiment with a unique value for the static suspension line length. In general, it was found that the heading rate is not strongly related to the static line length. In fact, the heading rate has a nearly linear relationship with normalized deflection of the dynamic line up until the point of saturation or canopy collapse. Although the achievable yaw rate is linearly related to control line deflection, the maximum and minimum yaw rates are dependent upon the static line deflection. By extension, if the heading rate is not significantly affected by changing the suspension line deflection, then the heading rate characteristics are not dependent on the glide ratio.

To develop, tune, and quantify the resulting performance of a heading stabilization controller, different tunnel speeds and different payload weights were used during the week-long testing event. The heading stabilization controller was characterized by analyzing the 190 individual experimental data sets.

As mentioned in Section 3, the controller developed during the vertical wind tunnel (VWT) test was then evaluated in the outdoor flight test conditions. As such, rather than discussing just the VWT results, the following discussion centers around comparing the controller developed during the VWT tests with the one further tuned during the outdoor flight test.

During the outdoor flight testing, the system was observed to be overexcited and the controller gains were reduced. The corresponding gains were reduced by approximately 50%; however, the proportionality between the three PID controller gains remained consistent. The resulting performance was more favorable and analysis of the flight data revealed a predictable scaled step input response to the vertical VWT test data. Results in Table 2 give the relevant characteristics for the performance of the developed controller both in the wind tunnel and in preliminary outdoor flight testing. The ability to quickly scale all of the controller gains to create a control system capable of following a desired heading without the need for excessive outdoor flight testing supports the conclusion that the controller developed in VWT tests is applicable under flight conditions.

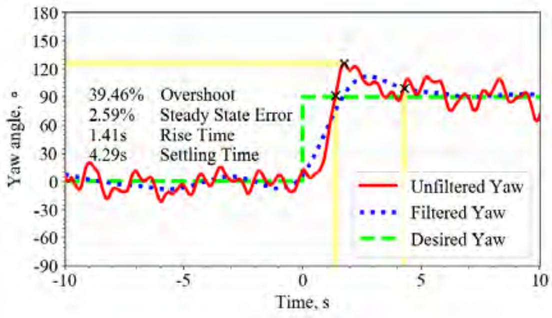

Fig. 6 : Example step response

Table 2: Performance of stabilization controller.

	VWT Tunnel	Flight Test	*Difference*
OS	71 %	34 %	52 %
e_{ss}	2.1 %	2.4 %	17 %
T_R	1.2 s	2.4 s	100 %
T_S	6.5 s	5.8 s	11 %

It is expected that the percent overshoot (OS) will be smaller and the rise time T_R will be larger for flight testing since the gains were reduced to alleviate over excitation and consequently the transient response is expected to be slowed. The relatively small values for steady state error(e_{ss}) support the conclusion that the steerable cruciform system is capable of precision navigation. Additionally, the close match between the flight test results and the VWT results further support the conclusion that the VWT experimental methodology closely mimics the dynamics of outdoor flight testing. Discrepancies could be due to the friction in the anchor/swivel mechanism in the wind tunnel.

Previously, the number experiments needed to successfully tune the controller gains was an obstacle to the development of a suitable controller. Even if the a controller developed at the VWT is not perfectly suited for flight testing, the ability to tune the system simply by scaling the magnitude of the three gains while keeping the proportion the same reduces the complexity and time associated with tuning the system for free-flight conditions.

In addition to tuning the heading controller, the collected test data was also used to identify the closed-loop dynamics of the yaw angle. The data used to identify the closed loop yaw model was first filtered with a cutoff frequency of 0.5 Hz. Filtering at such a slow frequency proved to be acceptable because the higher frequency information is not critical to characterize the motion of interest and is primarily a consequence of disturbances (wind, flexible fabric material, etc.). A potential challenge in utilizing the payload-sensed yaw angle is introduced by the relative motion between the payload and canopy. Using post-test photogrammetry analysis (discussed in Section 3.3) the relative motion was found to be as large as 20° at a frequency of 1 Hz. However, without a direct measurement of the canopy yaw angle, the parachute-payload is modeled as a single rigid body.

The second-order transfer function model structure was selected because it provided the closest match to the experimental data without over fitting. The input is the servoactuator command and the system output is the yaw angle. Consequently, the second-order transfer function model matches nicely with a basic intuitive understanding of the system physics. For a stable closed-loop system, it is expected that the input and output are separated by a time delay and some ripple in the magnitude. The general equation for the second order transfer function is given in Eq. (3).

$$H(s) = \frac{As+B}{s^2+Cs+D} \tag{3}$$

Several other model structures, including higher-order transfer functions and polynomial models were investigated. Over fitting was quantified by using the model created from a test data set to predict the output response from a verification data set and then comparing the predicted and measured outputs. The best model structure was selected by comparing the training and test error for various scenarios. The simple second-order transfer function structure represents the highest-order model which was not prone to overfitting the data. Average coefficients were estimated for one set of gains which showed the most favorable performance during the wind tunnel testing. Those coefficient are presented in Table 3. A sample plot showing measured yaw, filtered measured yaw and the yaw estimate from the identified model is shown in Fig. 7.

Table 3: Overall average coefficients for 2nd order transfer function model

Coefficient	Value
A	0.72
B	2.1
C	1.3
D	2.1

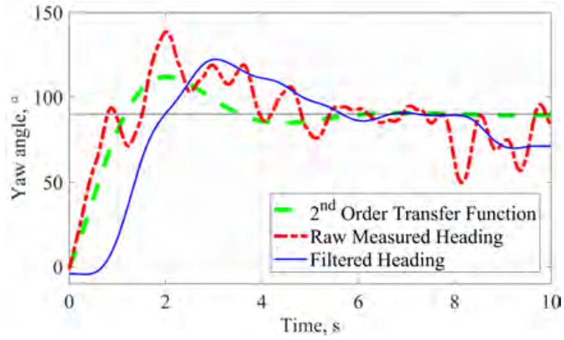

Fig. 7 : Comparison of measured and model-predicted yaw angle time histories

4.2 Glide Ratio Estimation

In addition to developing a heading controller and identifying the closed-loop dynamics, the VWT data were extended to approximate the glide ratio as a function of pitch angle. This estimation was performed by solving Eqs. (4) and (5) in order to find the canopy axial and side force respectively.

$$F_A = \frac{-m_p\left[\sin(q_1)(g - L_a u_1^2 - \dot{u}_2)\cos(q_1)\dot{u}_1\right]}{L_a + L_s} + \frac{m_p\left[\sin(q_1)(b^2 + h^2 + 12L_a^2)\cos(q_1)\dot{u}_1\right]}{L_a + L_s} \tag{4}$$

$$F_S = \frac{m_p\left[\cos(q_1)(g - L_a u_1^2 - \dot{u}2)\sin(q_1)\dot{u}_1\right]}{L_a + L_s} - \frac{m_p\left[\cos(q_1)(b^2 + h^2 + 12L_a^2)\sin(q_1)\dot{u}_1\right]}{L_a + L_s} \tag{5}$$

Determination of glide ratio is very important in terms of precision guidance capabilities, thus any method which enables glide ratio estimation from experiments conducted in the controlled VWT environment in an efficient manner provides a cost efficient yet data rich test program.

Data for the glide ratio model was filtered at 1.0 Hz. In this case, the low cutoff frequency is justified in the sense that the purpose of the glide ratio model is to capture the long-period gliding motion of the canopy and not the fast fluctuations associated with disturbances such as those due to the wind. Even if high frequency variations in the time signal are due to the actual motion of the system, removing this motion from the signal by filtering will have a small effect on the overall glide ratio estimate. A plot of glide ratio versus time for a typical experimental trial is shown in Fig. 8.

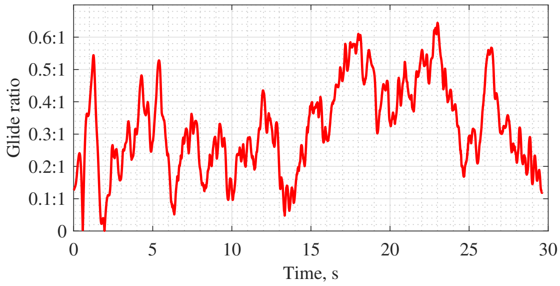

Fig. 8 : Typical instantaneous glide ratio calculated using data

Glide ratio for the steerable cruciform size/weight ranges used in this study have been experimentally determined previously to be 0.25 : 1 to 0.50 : 1 [9]. This is consistent with glide ratio estimates for similar canopies evaluated by Potvin et. al. [8]. As discussed by Fields and Yakimenko, the glide ratio estimate from outdoor flight testing is conservative because it does not account for inefficiencies associated with imperfect heading control including traversing along an oscillatory path [9].

Data from 90 VWT trials were collected and average glide ratio was computed. The resulting overall glide ratio for the VWT experiments was found to be 0.31 : 1. The glide ratio from the fixed heading outdoor flight tests was found to be 0.29 : 1. Thus, the simulation results in an estimate of glide ratio which is close to the glide ratio seen during flight testing. In fact, the simulated glide ratio is within about 7 % of the measured glide ratio from outdoor flight testing. Therefore, the VWT testing has the potential to be a fast and relatively simple means of estimating the glide ratio for low glide platforms like the steerable cruciform system.

4.3 Outdoor Flight Testing

Four separate outdoor flight test events were conducted in order to evaluate two different guidance paradigms. A summary of test events including maximum altitude and lifting platform is given in Table 4.

Table 4: Summary of Test Events

Location	Lifting platform	CARP Altitude (AGL)
Camp Roberts, CA	DJI M600	500 m
Camp Roberts, CA	GD X8	1900 m
Yuma, AZ	UH-60	1900 m
Eloy, AZ	Skyvan	1600 m

A plot of drop landing locations recorded at Camp Roberts for the PTT guidance scheme is shown in Fig. 10. The center of this plot represents the desired impact point for each individual drop. The blue markers represent the measured landing location for each individual parachute drop. This type of information was recorded for each of the testing events and used to generate the summary statistics shown in Table 5.

Though the miss distance is better for the WPN guidance technique, there are distinct dis-

Fig. 9 : UH-60 Blackhawk helicopter taking off

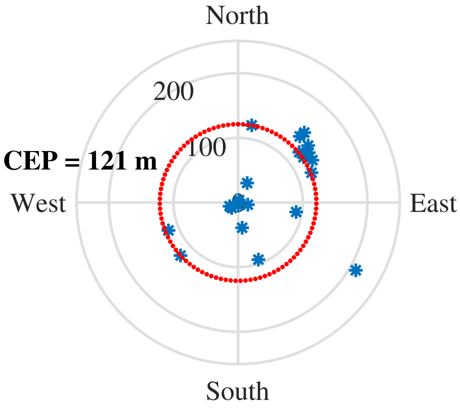

Fig. 10 : Camp Roberts PTT guidance results

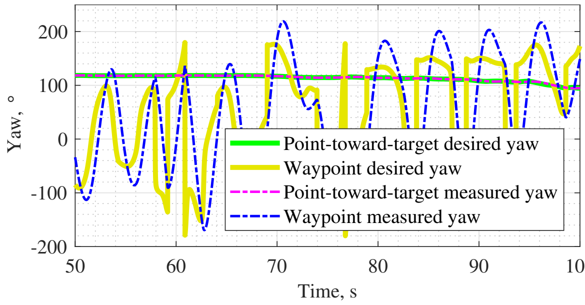

Fig. 11 : Comparison of desired and measured yaw angle for different guidance schemes

advantages to this approach. A plot showing typical measured and desired yaw for each of the two guidance strategies is shown in Fig. 11. Examining Fig. 11 it can be seen that the desired yaw angle is over excited when the system draws close to and overtakes a waypoint. While it is true that the yaw is filtered according to the system dynamics, there is still oscillation present in the heading. This oscillation effectively wastes the already limited glide capability of the system. Conversely, though the PTT guidance scheme results in a larger miss distance, the desired heading is mostly smooth and thus results in a trajectory which uses the gliding capability of the system more effectively and is more efficient in terms of controller actuation.

Table 5: Outdoor flight test results

Event	**Strategy**	**CEP** m
Overall	Combined	64
Camp Roberts, CA	Combined	67
Camp Roberts, CA	WPN	14
Camp Roberts, CA	PTT	122
Yuma Proving Ground	PTT	2
Eloy, AZ	PTT	98

5 Conclusions

A cruciform parachute has been developed, tuned, and tested in both a vertical wind tunnel and through outdoor flight tests. The vertical wind tunnel provided an efficient test platform for tuning the heading stabilization controller for the cruciform parachute. Additionally, the glide ratio was readily estimated from the already collected wind tunnel data, and results indicate strong agreement between the model and data collected during outdoor gliding flight tests. Outdoor flight tests were conducted from a variety of deployment platforms and altitudes, and the results demonstrate the capability for semi-precision aerial delivery. The persistent point-toward-target technique utilizes the most gliding capability of the parachute system, but is susceptible to overshooting the desired impact point due to uncertainty in the forecast of the surface winds. The waypoint guidance scheme utilizes forecast winds to generate the desired path, and the limited results indicate good landing accuracy when the predicted wind conditions are at least moderately accurate. Overall, the developed steerable cruciform parachute system presents a novel low-cost but yet effective precision aerial delivery means that has the potential to fill a much needed gap between low-cost unguided delivery systems and high-cost ram-air parafoil systems.

References

[1] Oleg A Yakimenko, editor. *Precision Aerial Delivery Systems: Modeling, Dynamics, and Control*. AIAA Progress in Astronautics and Aeronautics, Arlington, VA, 2015.

[2] Forichon Alphonse. Parachute, August 22 1961. US Patent 2,997,263.

[3] Ron J Niccum, Eugene L Haak, and Robert Gutenkauf. Drag and stability of cross type parachutes. Technical report, University of Minnesota, Minneapolis, MN, 1965.

[4] William P Ludtke. Effects of canopy geometry on the spinning characteristics of a cross parachute with a w/l ratio of 0.264. Technical report, Naval Ordnance Lab White Oak MD, Jun 1972.

[5] Dean Stafford Jorgensen. *Cruciform parachute aerodynamics*. PhD thesis, University of Leicester, 1982.

[6] CQ Shen and DJ Cockrell. Aerodynamic characteristics and flow round cross parachutes in steady motion. *Journal of Aircraft*, 25(4):317–323, 1988.

[7] D Levin and Z Shpund. Canopy geometry effect on the aerodynamic behavior of

cross-type parachutes. *Journal of Aircraft*, 34(5):648–652, 1997.

[8] Jean Potvin, Jason Papke, Eric Brighton, Tobia Hawthorne, Gary Peek, and Richard Benney. Glide performance study of standard and hybrid cruciform parachutes. In *Proceedings of the 17th AIAA Aerodynamic Decelerator Systems Technology Conference and Seminar*, volume 2160. AIAA, 2003.

[9] Travis D Fields and Oleg A Yakimenko. Development of a steerable single-actuator cruciform parachute. *Journal of Aircraft*, pages 1–9, 2017.

6 Contact Author Email Address

For correspondence regarding the manuscript please contact Travis Fields at fieldstd@umkc.edu.

Copyright Statement